GROUND DISPLACEMENT MEASUREMENT OF THE 2013 M7.7 AND M6.8 BALOCHISTAN EARTHQUAKE WITH TERRASAR-X SCANSAR DATA

Nestor Yague-Martinez[1,5], Eric Fielding[2], Mahmud Haghshenas-Haghighi[3], Xiao Ying Cong[1], Mahdi Motagh[3], Ulrich Steinbrecher[4], Michael Eineder[5], Thomas Fritz[5]

[1] Chair of Remote Sensing Technology, Technische Universität München. Munich, Germany.
[2] Jet Propulsion Laboratory, California Institute of Technology. Pasadena, California, USA
[3] GFZ German Research Center for Geosciences, 14473 Potsdam, Germany.
[4] Microwaves and Radar Institute, German Aerospace Center. Weßling, Germany.
[5] Remote Sensing Technology Institute, German Aerospace Center. Weßling, Germany.

ABSTRACT

This paper addresses the November 2013 Balochistan Earthquake. A co-seismic TerraSAR-X pair acquired in wide-swath ScanSAR mode has been used to derive two-dimensional deformation measurements (radar line-of-sight and azimuth direction) of the eastern part of the main M7.7 earthquake and the large M6.8 aftershock by correlating SAR amplitude images. Atmospheric and solid Earth tide corrections have been considered to achieve accuracy in the order of several centimeters. Correlation measurements from Landsat-8 images have been additionally estimated. The intention is to isolate vertical and horizontal components in order to obtain three-dimensional deformation measurements. Interferometric processing issues of ScanSAR data for non-stationary scenarios, specifically co-registration, are additionally discussed.

Index Terms— Earthquakes, InSAR, correlation, Balochistan, ScanSAR.

1. INTRODUCTION

The September 24, 2013 a M7.7 earthquake in south-western Pakistan occurred as the result of oblique-strike-slip type motion at shallow crustal depths. The epicenter of the event is located 69 km north of Awaran, Pakistan, and 270 km north of Karachi, Pakistan. An aftershock of M6.8 occurred four days later 30 km to the north-northeast, which struck with a similar faulting mechanism [1].

Avouac et al.[2] have used satellite optical data and teleseismic waveforms to study this earthquake. Jolivet et al.[3] have additionally used satellite radar images to retrieve the surface displacement. They used a pair of Radarsat-2 images, which cover the south-east part of the surface rupture, and two TerraSAR-X stripmap pairs, in descending geometry, covering the center and the north-east parts. In this paper we used two pairs of Landsat-8 images to derive a horizontal displacement map and a pair of TerraSAR-X ScanSAR images in ascending geometry with a range coverage of approx. 100 Km and azimuth coverage of approx. 400 Km.

2. DATA

2.1 TerraSAR-X ScanSAR data. Burst synchronization

A TerraSAR-X ScanSAR image acquired with the satellite TDX-1 on the 21.11.2011 in ascending geometry with incidence angles ranging from 31.6° to 40.6° over the eastern part of the affected area was available in the TerraSAR-X catalogue. ScanSAR acquisitions contain only a portion of the total azimuth bandwidth for a certain scatterer. Interferometry can only be performed if enough Doppler spectrum overlap is present, therefore burst synchronization is required. The two satellites TSX-1 and TDX-1 performing the TerraSAR-X mission are applying a Datatake start strategy by orbit position, not only by orbit time, enabling the start of Datatakes at nearly the same orbit position in flight direction relative to Earth. Since TSX-1 shall fly always its constant reference orbit, the same order input would lead to the same burst synchronous Datatake. However TDX-1 flies a variable distance circling around the TSX-1 (TanDEM-X mission helix formation) which may lead to a slightly different Datatake, even with identical order input. PRF changes of some Hz and changes in burst length of even +/- 1 pulse would destroy the interferometric required burst synchronism. With a special commanding, called System Datataking, the second acquisition was forced to have the same parameters than the first acquisition. The second acquisition took place on the 25.10.2013 with the TDX-1 satellite, resulting in a pair of burst synchronous ScanSAR Datatakes, with only a slight (some 100m) difference in range, which is covered by the range overlap between the subswathes of about 1 Km. The mutual along-track deviation is only 71.5 m. This provides (together with the Doppler centroid differences of both acquisitions) a

burst synchronism of around 80% (common Doppler bandwidth of both acquisitions is 380 Hz of a total available bandwidth of 475 Hz). The co-seismic TerraSAR-X ScanSAR pair includes the M7.7 main shock as well as the M6.8 aftershock.

2.2. Landsat-8 data

Two pairs of Landsat 8 images (path 154, row 41 and row 42) were used for the processing. The pre-earthquake and post-earthquake images have been acquired on 10 September 2013 and 26 September 2013 respectively. Therefore the Landsat 8 results cover uniquely the M7.7 shock. The images are in panchromatic bands (15m resolution).

3. METHODOLOGY

This section provides the methodology for the interferometric processing of TerraSAR-X ScanSAR data. The derivation of absolute displacements from ScanSAR data employing correlation techniques and correcting for geodynamical effects is also described. Finally the procedure to obtain a horizontal displacement map from Landsat-8 images is explained.

3.1. ScanSAR Interferometric Processing issues

The algorithms for the interferometric processing of TerraSAR-X burst-mode data with the operational Integrated TanDEM-X Processor (ITP) are provided in [4]. A critical operation for the interferometric processing of burst-mode data is the azimuth co-registration. Scheiber and Moreira [5] have performed an analysis of the phase bias introduced due to a misregistration in the case of squinted acquisitions. For the case of a varying Doppler centroid frequency over azimuth, a phase ramp appears if a constant misregistration is present. The necessary azimuth co-registration accuracy for TerraSAR-X ScanSAR is 0.004 pixels, or 3.3 cm (if an interferometric phase error of 3° is allowed [4]). If no deformation is expected and the orbits of both acquisitions are parallel, a correction of the geometric estimates with a constant value retrieved from the signal, as proposed in [6], provides very good results. In our scenario the surface rupture line crosses the scene, presenting in this way different azimuth shifts on two separated regions. A more complex correction model is then necessary. The model parameters have been derived exploiting the azimuth shifts from the incoherent cross-correlation.

3.2. Deformation map with TerraSAR-X ScanSAR images using correlation techniques

The method used to derive the two-dimensional deformation map is based on cross-correlation of the mosaicked ScanSAR amplitudes in the radar coordinates domain. Patches of size 512 (rg) x 128 (az) pixels (~700 m x 900 m) distributed regularly over a grid whose centers are separated by 64 pixels (~ 90 m in range and 450 m in azimuth) have been used. The differential atmospheric path delay has been computed using global weather model data from the European Centre for Medium-Range Weather Forecast (ECMWF). Solid Earth tide corrections have been applied. More details on this procedure can be found in [7] and [8].
The accuracy of cross-correlation applied to detected circular complex Gaussian signals has been provided by De Zan [9]. Figure 1 shows the corresponding standard deviation for range and azimuth directions using the previous parameters. Observe that the accuracy in azimuth is worse than in range due to its reduced resolution.

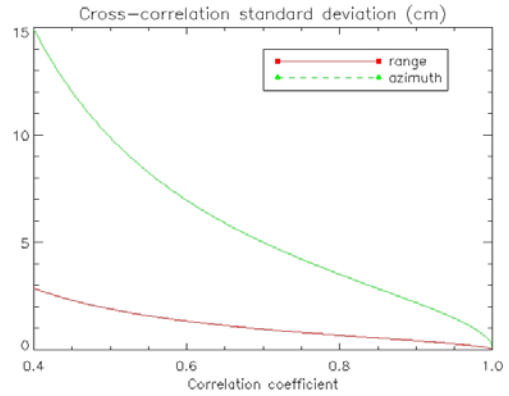

Figure 1 Plot of the incoherent cross-correlation standard deviation for range and azimuth direction assuming circular complex Gaussian signals (Correlation patch size is 512 x 128 pixels, pixel spacing are 1.36 m in range and 7.09 m in azimuth).

3.3. Deformation map with Landsat-8 images using correlation techniques

We used the Caltech COSI-Corr software package (methodology can be found in [10]) to do sub-pixel correlation and extract the horizontal components of surface displacements from two pairs of Landsat-8 images. The images are correlated in frequency domain with a window size of 64x64 pixels (~ 960 x 960 m). The distance between patches is 32 pixels (~ 480 m). Parallel strip artifacts have been removed in a two-step process: firstly the main co-seismic displacement map was masked out around the surface rupture area to better estimate stripping effect. Secondly, the mean of all remaining pixels in both, E/W and N/S directions, were estimated and subtracted from all pixels in the displacement map.
A mosaicking of the displacement maps of both adjacent frames has also been performed, the displacement in the overlap area has been averaged. Finally a moving average filtering has been applied to reduce remaining noise.

4. RESULTS AND INTERPRETATION

Fig 2 shows a Google Earth visualization of the TerraSAR-X ScanSAR differential interferometric wrapped phase and the Landsat 8 images coverage. Fig. 3 shows a map of the TerraSAR-X range (LOS) displacements with the location of the M7.7 surface ruptures mapped by Avouac et al.[2] The TSX LOS vector has an azimuth of 78.8° and varying incidence angle across the scene from 31.6° on the western edge to 40.6° on the eastern edge, and negative displacement means motion towards the satellite (west and up). Fig. 4 shows the predicted surface displacements from the Avouac et al.[2] static slip model, projected into the TSX LOS direction at a constant incidence angle of 36° (average for the swath). Fig 5 shows the absolute displacement map from correlating the Landsat-8 images. The interpretation of the TSX ScanSAR interferogram indicates that the M6.8 aftershock ruptured a part of the fault system that had less slip in the M7.7 main earthquake.

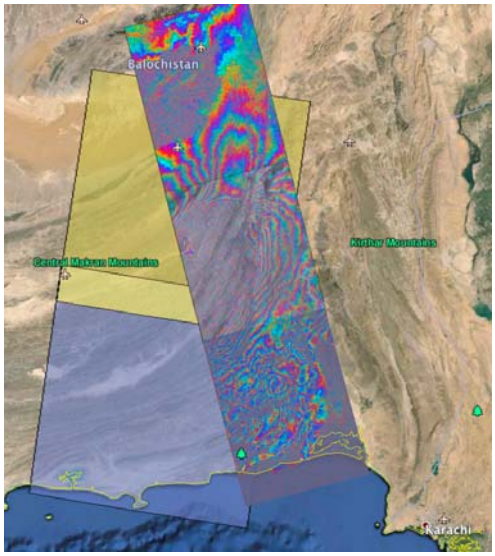

Figure 2 Visualization on GoogleEarth of the TerraSAR-X ScanSAR differential phase (mosaick of three scenes, containing each 4 subswaths, 55 bursts / subswath). Each fringe is 1.55 cm of ground displacement in the radar line of sight. Extension: 100 km x 400 km. A SRTM DEM has been subtracted from the interferometric phase. Landsat 8 images coverage, path 154 row 41 (yellow) and row 42 (blue) are as well shown.

Some of the differences between the predicted and observed displacements are due to the varying incidence angle, but this is a minor effect. The substantially greater extent of the observed large LOS displacements is likely due to incorrect fault geometry and slip distribution in the northern part of the Avouac et al.[2] fault slip model, which was estimated only from the horizontal displacements derived from the Landsat-8 data (similar to Fig. 5).

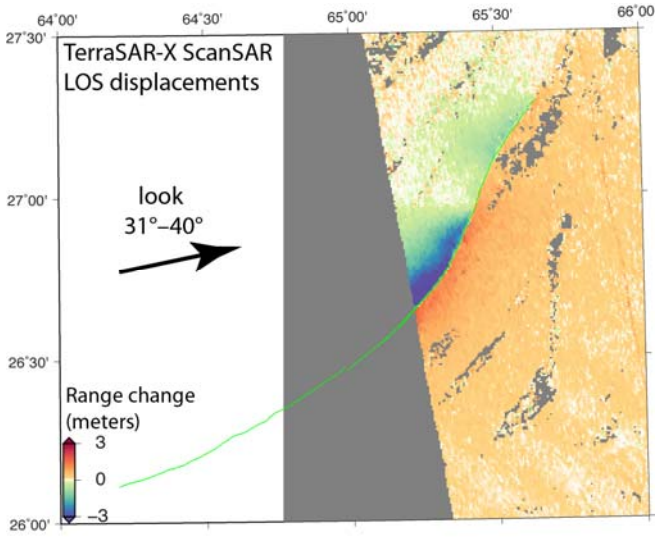

Figure 3 Displacements measured from correlation shifts in the range (LOS) direction from TerraSAR-X ascending track data. Incidence angle varies across the radar scene. Green line is surface rupture interpreted from Landsat-8 shift map [2].

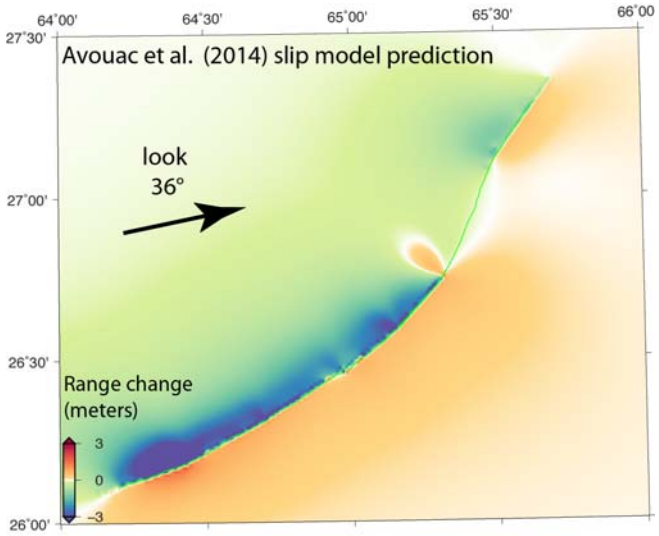

Figure 4 Predicted displacements from the Avouac et al. [2] static fault slip model projected into the TerraSAR-X ascending track LOS direction at a constant incidence angle (mid-range). Green line is same surface rupture interpreted from Landsat-8 shift map[2]

The TSX LOS displacements provide additional information on the vertical component of surface motion that improves the estimates of fault slip from this earthquake, as shown by Jolivet et al.[3] who used LOS displacements from the TSX stripmap images covering a much smaller part of the rupture than the TSX ScanSAR data. A small amount of the difference can be due to the surface displacements during the M6.8 aftershock, but these displacements are much

smaller than the much larger M7.7 mainshock. It is likely that the M6.8 aftershock ruptured the northern part of the fault system that had less slip in the M7.7 main earthquake, but additional analysis is necessary to separate the smaller aftershock displacements from the mainshock displacements in the TSX interferogram and shift measurements.

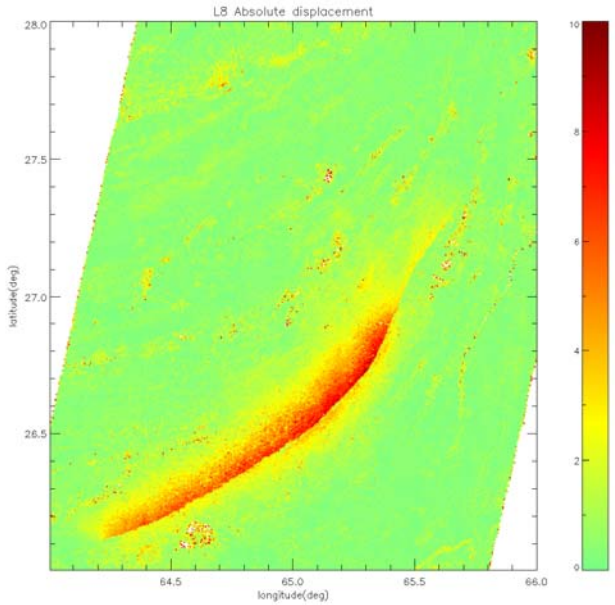

Figure 5: Surface absolute displacement map derived from correlating co-seismic Landsat-8 images.

4. CONCLUSSIONS

In this paper we used TerraSAR-X ScanSAR co-seismic images of the Balochistan Earthquake to derive displacement maps by employing correlation techniques and applying geodynamic corrections to the derived shifts. The necessity of burst synchronism for ScanSAR data has been justified for interferometry. The suitability of the TerraSAR-X system to achieve good burst synchronism has been demonstrated. Landsat-8 images have been also used to derive two-dimensional horizontal displacements and a displacement map of the absolute displacement has been given. The derived TerraSAR-X displacement map in the line-of-sight has been compared with predicted shifts of the slip model performed by Avouac et al.[2] projected into the TerraSAR-X ascending range direction at the mid-range incidence angle. Some significant differences between the prediction of the model and the TSX displacement maps can be observed probably because their inversion only used the horizontal displacements from Landsat-8 images.

In a future publication we will provide a 3D displacement map by combining horizontal measurements from Landsat-8 and measurements in the LOS from TerraSAR-X.

ACKNOWLEDGMENTS

The TerraSAR-X ScanSAR data has been provided by the German Aerospace Center, DLR (Proposal number MTH-0404). Landsat-8 data was provided by the US Geological Survey EROS Data Center. We thank Shengji Wei for providing the predicted static displacements calculated from the fault slip model of Avouac et al[2]. Part of this research was supported by the NASA Earth Surface and Interior focus area and performed at the Jet Propulsion Laboratory, California Institute of Technology.

REFERENCES

[1] U.S. Geological Survey: http://comcat.cr.usgs.gov/earthquakes/eventpage/usb000jyiv#summary and http://comcat.cr.usgs.gov/earthquakes/eventpage/usb000k1gb#summary

[2] J. P. Avouac, F. Ayoub, S. Wei, J. P. Ampuero, L. Meng, S. Leprince, R. Jolivet, Z. Duputel. The 2013, MwBalochistan earthquake, energetic strike-slip reactivation of a thrust fault. Earth and Planetary Science Letters 391 (2014) 128-134

[3] R. Jolivet, Z. Duputel, B.Riel, M. Simons, L. Rivera, S.E. Minson, H. Zhang, M. A. G. Aizavis, F. Ayoub, S. Leprince, S. Samsonov, M. Motagh and E. Fielding. The 2013 Mw 7.7 Balochistan Earthquake: Seismic Potential of an Accretionary Wedge.

[4] N. Yague-Martinez, F. Rodriguez-Gonzalez, U. Balss, H. Breit, T. Fritz. TerraSAR-X TOPS, ScanSAR and WideScanSAR interferometric processing. EUSAR 21014 Workshop. June 2014, Berlin.

[5] R. Scheiber and A. Moreira. Coregistration of Interferometric SAR Images Using Spectral Diversity. IEEE Transactions on Geoscience and Remote Sensing, Vol. 38, No. 5, September 2000, pp 2179-2191.

[6] P. Prats-Iraola, R. Scheiber, L. Marotti, S.Wollstadt and A. Reigber. TOPS Interferometry with TerraSAR-X, IEEE TGRS. Vol. 50, No. 8, August 2012, pp 3179-3188.

[7] N. Yague-Martinez, M. Eineder, X.Y. Cong, C. Minet. Ground displacement Measurement by TerraSAR-X Image Correlation: The 2011 Tohoku-Oki Earthquake. IEEE GRSL, Vol. 9, No. 4, pp.539-543, July 2012.

[8] X. Cong, U. Balss, M. Eineder, T. Fritz. Imaging Geodesy - Centimeter-Level Ranging Accuracy With TerraSAR-X: An Update. IEEE GRSL, Vol. 9, No. 5, pp. 948-952, September 2012.

[9] F. de Zan. Accuracy of Incoherent Speckle Tracking for circular Gaussian Signals. IEEE Geoscience and Remote Sensing Letters. IEEE GRSL, Vol. 11, No. 1, pp.264-267. January 2014.

[10] S. Leprince, S. Barbot, F. Ayoub and J. P. Avouac. Automatic and Precise Ortho-rectification, Coregistration, and Subpixel Correlation of Satellite Images, Application to Ground Deformation Measurements", IEEE TGRS, vol. 45, no. 6, pp. 1529-1558, 2007.